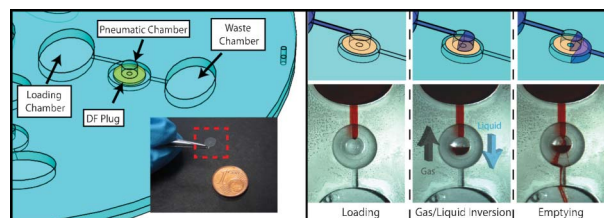# Lab on a Chip

Centrifugo-pneumatic valving utilizing dissolvable films

Robert Gorkin III,* Charles Nwankire, Jennifer Gaughran, Xin Zhang, Gerard G. Donohoe, Martha Rook, Richard O'Kennedy and Jens Ducrée

We demonstrate novel valving based on dissolvable films in centrifugal microfluidics. Focus is on mechanical validation, film biocompatibility, and sequential processing for potential automation of biochemical assay protocols.

2

Please check this proof carefully. Our staff will not read it in detail after you have returned it.

Translation errors between word-processor files and typesetting systems can occur so the whole proof needs to be read. Please pay particular attention to: tabulated material; equations; numerical data; figures and graphics; and references. If you have not already indicated the corresponding author(s) please mark their name(s) with an asterisk. Please e-mail a list of corrections or the PDF with electronic notes attached — do not change the text within the PDF file or send a revised manuscript.

Please bear in mind that minor layout improvements, e.g. in line breaking, table widths and graphic placement, are routinely applied to the final version.

We will publish articles on the web as soon as possible after receiving your corrections; no late corrections will be made.

Please return your **final** corrections, where possible within **48 hours** of receipt, by e-mail to: loc@rsc.org

Electronic (PDF) reprints will be provided free of charge to the corresponding author. Enquiries about purchasing paper reprints should be addressed via: http://www.rsc.org/publishing/journals/guidelines/paperreprints. Costs for reprints are below:

Reprint costs

No of pages	Cost for 50 copies	Cost for each additional 50 copies
2–4	£225	£125
5–8	£350	£240
9–20	£675	£550
21–40	£1250	£975
>40	£1850	£1550

Cost for including cover of journal issue:
£55 per 50 copies

Authors Queries

Editor's queries are marked like this... ☐1, and for your convenience line numbers are indicated like this... 5.

Query Reference	Query	Remarks
1	[INFO-1] Please carefully check the spelling of all author names. This is important for the correct indexing and future citation of your article. No late corrections can be made. FOR YOUR INFORMATION: You can cite this paper before the page numbers are assigned with: (authors), Lab Chip, DOI: 10.1039/c2lc20973j.	
2	Is the contents entry acceptable? The descriptive text should be no longer than 30 words. If the entry does not fit between the two horizontal lines, then please trim the text and/or the title.	
3	Should there be supplementary data associated with this article? We do not appear to have received any.	

Centrifugo-pneumatic valving utilizing dissolvable films

Robert Gorkin III,*[ab] Charles Nwankire,[ab] Jennifer Gaughran,[ab] Xin Zhang,[ac] Gerard G. Donohoe,[d] Martha Rook,[d] Richard O'Kennedy[ac] and Jens Ducrée[ab]

In this article we introduce a novel technology that utilizes specialized water dissolvable thin films for valving in centrifugal microfluidic systems. In previous work (William Meathrel and Cathy Moritz, *IVD Technologies*, 2007), dissolvable films (DFs) have been assembled in laminar flow devices to form efficient sacrificial valves where DFs simply open by direct contact with liquid. Here, we build on the original DF valving scheme to leverage sophisticated, merely rotationally actuated vapour barriers and flow control for enabling comprehensive assay integration with low-complexity instrumentation on "lab-on-a-disc" platforms. The advanced sacrificial valving function is achieved by creating an inverted gas-liquid stack upstream of the DF during priming of the system. At low rotational speeds, a pocket of trapped air prevents a surface-tension stabilized liquid plug from wetting the DF membrane. However, high-speed rotation disrupts the metastable gas/liquid interface to wet the DF and thus open the valve. By judicious choice of the radial position and geometry of the valve, the burst frequency can be tuned over a wide range of rotational speeds nearly 10 times greater than those attained by common capillary burst valves based on hydrophobic constrictions. The broad range of reproducible burst frequencies of the DF valves bears the potential for full integration and automation of comprehensive, multi-step biochemical assay protocols. In this report we demonstrate DF valving, discuss the biocompatibility of using the films, and show a potential sequential valving system including the on-demand release of on-board stored liquid reagents, fast centrifugal sedimentation and vigorous mixing; thus providing a viable basis for use in lab-on-a-disc platforms for point-of-care diagnostics and other life science applications.

1. Introduction

Robust valving over a wide range of rotational burst frequencies is pivotal for developing highly integrated centrifugal microfluidic platforms for advanced clinical analysis.[2,3] Valving structures are fundamental in enabling sequential fluidic processing required for intricate assays, and typically assay protocols rely on key fluidic elements (*e.g.*, decanting, metering, mixing, siphoning) that are either derived from or can be improved through valving technologies.[4–8] In the disc format, the assay fluidics are multiplexed and, as such, several valving components must work simultaneously.[9] Fundamentally valving issues become more complex when used within the area of clinical diagnostics; valves must be compatible to common manufacturing schemes of the testing device, in addition, they must be actuated in accordance with the design paradigms of the instrument, and furthermore, they must provide long-term

stability to address the important topics of on-board liquid reagent storage and the prevention of cross-contamination.

In a common arrangement, valving in centrifugal microfluidics has taken the form of constrictions in microchannels, whereby liquids driven outwards by centrifugal forces are prevented from flowing due to opposing surface tension created at the interface (this can be termed a passive valve). The valve holds until spin velocities, measured in rotations per minute (RPMs), are increased above a critical threshold, known as the burst frequency. In native polymers and on (locally) deposited hydrophobic layers, these structures are called hydrophobic valves.[10] While comparatively easy to fabricate, hydrophobic valves have a limited gamut of use. Their operational band of rotational burst frequencies is quite narrow and scales only linearly with radial position on the disc. As such, only simple disc designs utilizing a few valves, and thus limited sequential assay steps, are possible as rotational frequency bands start to overlap and cause unwanted valving failures. Furthermore, for a given valve design, the burst frequency decreases with increasing distance away from the disc centre. This characteristic that valves would yield first near the edge and then near the centre of the disc contradicts the design paradigm of centrifugal systems where samples are introduced near the disc centre and are then

[a] *Biomedical Diagnostics Institute, National Centre for Sensor Research, Dublin City University, Glasnevin, Dublin 9, IRELAND. E-mail: Robert Gorkin robertgorkiniii@gmail.com; Jens Ducrée jens.ducree@dcu.ie*
[b] *School of Physics, Dublin City University, Dublin 9, IRELAND*
[c] *School of Biotechnology, Dublin City University, Dublin 9, IRELAND*
[d] *EMD Millipore, 80 Ashby Road, Bedford, MA, USA*

sequentially driven through the processing chambers for analysis towards the perimeter of the disc.

More recently, sacrificial valves were introduced to overcome the limitations of passive valving and to increase centrifugal microfluidic capabilities for expanded use. Serving as superior liquid/vapour barriers, sacrificial valves act as programmable flow control elements where a physical gating material is changed or removed by an external actuation source. Wax valving using native compositions of different temperature waxes has been shown using focused IR lamp sources as the actuator.[12] Another prominent example is a sacrificial valving technology utilizes ferrowax impregnated with infrared (IR) absorbing nanoparticles which are actuated by laser diodes.[11] Additionally optofluidic valves have been developed where *cyclo*-olefin polymer (COP) and polyethylene terephthalate (PET) films spotted with heat absorbing printer toner could be ablated using laser diodes.[12] Such active valves allow for the increase in the number of processes that can be independently controlled on a single disc.[8,13] The use of these sacrificial valves lessens the restraints due to operational frequency range since they are not reliant on rotational frequency to open. However, while superior in their flexibility of flow control, the fact that sacrificial valves necessitate embedding a barrier material and actuating those gating mechanisms through rather complex external actuation units and trigger control (to be azimuthally synchronised with the rotational motion) poses severe challenges to manufacturing and instrumentation.

In the latest evolution of valving technology on a disc, new concepts have been developed that retain the liquid and vapour barrier properties of sacrificial valves, while at the same time the valves are actuated without the need for peripheral equipment (other than the platform-immanent spindle motor). Two notable examples based on a similar concept are the burstable foil seal valves from Hoffman *et al.*[14] and the elastomeric membrane valves by Hwang *et al.*[15] Both groups introduced a weakly bonded flexible barrier in a microchannel that was actuated entirely *via* the frequency of rotation. Pressures introduced by the liquids during centrifugation deformed the foil/membrane, thereby allowing for liquid to pass through the valve site. While these valves show an improvement in centrifugal microfluidic operation, their use may be restricted as they operate only at low spin speeds and also introduce manufacturing complexity to the system.

Here we report for the first time on a novel concept describing valving based on water-soluble films. The material choice coupled with a unique chamber design enables a new variant on centrifugo-pneumatic flow control, which, dramatically increases the working range of the burst frequencies as compared to purely surface-tension derived valving while eliminating the need for peripheral actuation mechanisms like laser sources as previously described for the phase-change wax valves. Additionally, the simple, lamination-based fabrication technique has the potential to provide a novel active valving mechanism that provides the strength of a physical barrier in a manner that easily integrates with commercial production techniques.

This paper commences with the concept of dissolvable film (DF) based valving, followed by a detailed examination of our refinements for an advanced centrifugo-pneumatic flow control succeeded by an experimental validation and evaluation of the system. In order to complete the discussion of valving for use in real-world life-science applications, the next section provides an analysis on the compatibility of the films in bioassays. Finally, we will also demonstrate applications for advanced control of fluidic processes enabled by the use of the valves. Overall the report reveals the potential for dissolvable film valving in centrifugal microfluidics.

2. Design of dissolvable film valves

The fundamental concept underlying our system is the interaction of liquids with a DF barrier. When a liquid is introduced to the DF surface, the film begins to breakdown, eventually disintegrating and allowing liquids to pass through the valve opening. However, standalone films cannot be used for valving as they lack the ability to be embedded in microfluidic devices. In order to overcome this limitation, a valving "tab" is assembled using multifunctional adhesive film technology to form a supporting structure for the DF, and to enable simple placement inside micro fluidic systems. To fabricate the plugs, two materials are used: the first layer contains pressure sensitive adhesives (PSA films) whereas the second layer consists of a specialized DF membrane. Inserting the tabs (Fig. 1) to restrict the microfluidic pathway creates the transient physical barriers for the valving; the tacky nature of the PSA films allows for closing off microchannels by merely sticking the plugs into the system features.

The DFs are derived from an aqueous polymer matrix consisting of a range of constituents such as various cellulose derivatives, hydrocolloids, acrylate copolymers, gums, polysaccharides and plasticizers. The dissolution times of the DFs
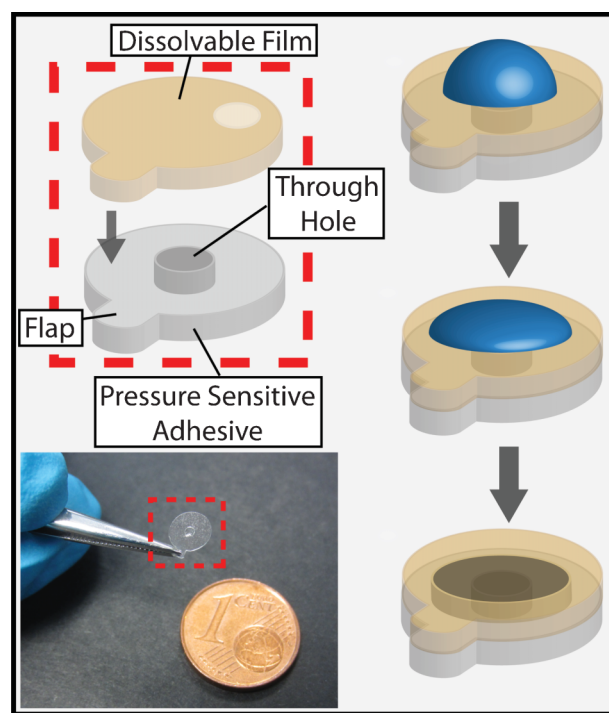

Fig. 1 Assembly of a valving tab consisting of a dissolvable film and a pressure sensitive adhesive. As liquid wets the surface, the film starts to deteriorate, eventually completely dissolving the barrier. The structure allows for fluid movement through the remaining feature.

depend on the specific mixture of the constituents.[1,16] In the current demonstrations two commercially available films were tested: one rated as a quick dissolution film (~ 10 s) and one rated as a slow dissolving film (~ 5 min).

3. Centrifugo-pneumatic valving

3.1 Concept

DFs can be used to enhance valving in centrifugal microfluidics; the current architecture expands on the established centrifugo-pneumatic valving concept. Fig. 2A illustrates the design of the system where a valving tab is embedded into a specially devised microchannel conduit. This tab is placed on the bottom of an air ballast chamber that is positioned between the loading and waste chambers. While still intact, the tabs form a fluid barrier sealing off a through hole connecting the two fluidic layers (Fig. 2B). After the introduction of the liquids into the loading chamber and priming of the microchannels, typically at low rotational speeds, a gas pocket forms above the tab. The action of the liquid traps the air, and the gas pocket prevents any further movement of the liquid. Akin to the pneumatic valving mechanism described in Mark *et al.*,[17] the balance of the pressure in the gas pocket and the centrifugally induced hydrostatic pressure exerted by the liquid plug halts the flow. The valve then follows a two-step actuation process. First, the valve will remain closed until spinning rates are increased to a critical rotational frequency at which the inverted liquid-gas stack destabilizes, causing the liquid to enter the air ballast chamber and wetting the film. Second, as fluids are pumped to the interface, the film rapidly liquefies and the valve fully opens. Continuously applied centrifugal force then propels the liquid through the valve opening into the exit microchannel. Fig. 2C shows an image series of the valve in action. For clarity, as both the liquid inversion and the film dissolution occur at the same critical spin speed, the more traditional notion of a ''burst frequency'' will be expanded to describe two-step valving actuation in this report.

3.2 Valving mechanics

As outlined, the valving mechanism depends on the balance between the centrifugally induced pressure head Δp and a critical yield pressure p_{crit} which needs to be determined experimentally. Qualitative measurements provide strong evidence that the critical yield pressure is dependent on the volume of the air-filled chamber on top of the DF membrane and the detailed contour of the expansion of the channel into the DF chamber. The centrifugally induced pressure

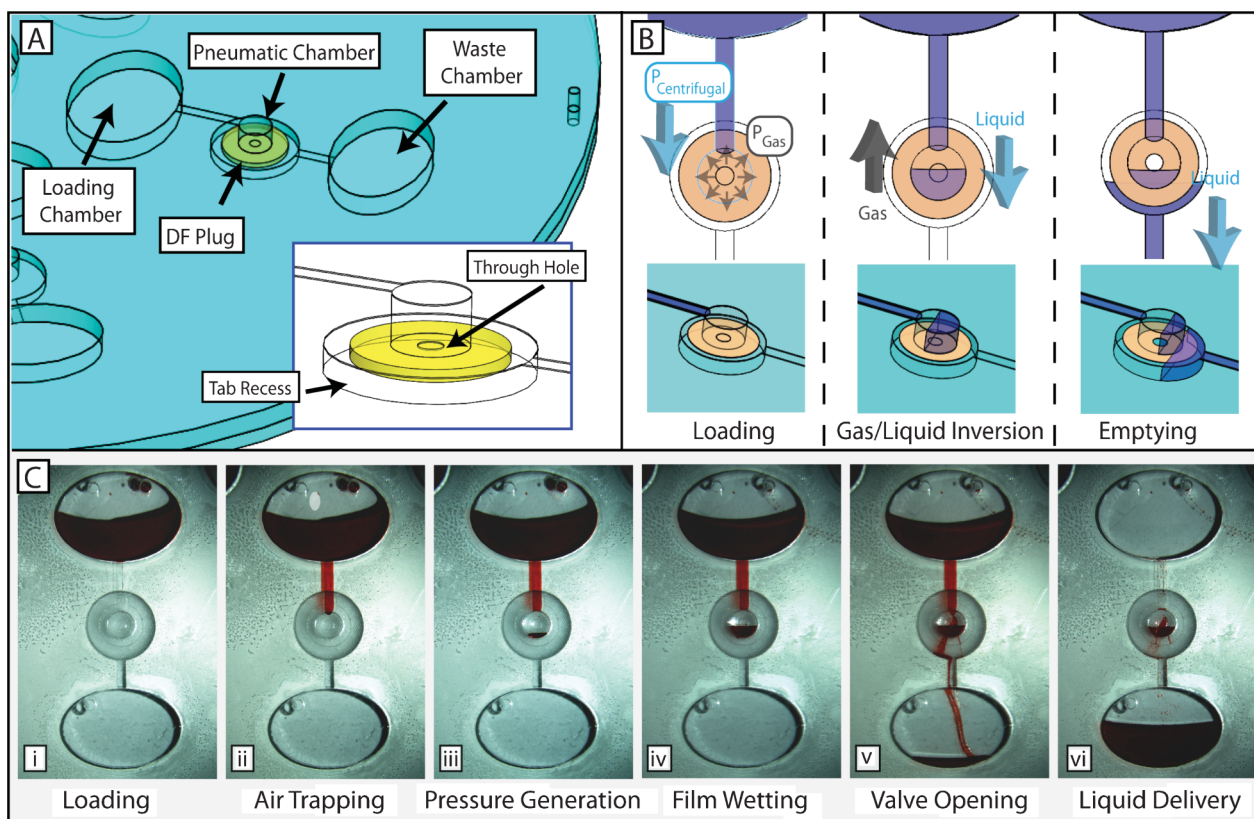$$\Delta p_\omega = \rho \Delta r \bar{r} \omega^2 \qquad (1)$$

Fig. 2 Centrifugo-pneumatic valving demonstration. A) Schematic diagram that illustrates the centrifugo-pneumatic valving concept. Inset shows a picture of the valving tab placement B) Principle of operation at the point of loading, during gas/liquid inversion and after film dissolution and emptying of the sample fluid. C) Image series of valving in action i–ii) Sample loading and air ballast trapping take place at low spin speeds (500 RPM– 3500 RPM). iii) Increased rotational frequencies induce air compression and air/fluid inversion in the chamber. iv) Introduction of liquids leads to disintegration of the DF and valve opening (4000 RPM). v–vi) Continued rotation facilitates emptying.

scales with the density ρ, the radial length Δr and the mean position $\bar{r}$ of the liquid plug spinning at the angular frequency ω.

The protruding meniscus stops as Δp_ω is balanced by pressure in the valve chamber

$$p = p_0 \frac{1}{1 - \Delta V / V_0} \qquad (2)$$

As derived from Boyle's law. In (2) p_0 represents the ambient pressure, V_0 is the (full) chamber volume initially available to the gas pocket and ΔV is the (gas) volume reduction due to the advancing liquid meniscus.

The liquid-gas interface in this metastable, inverted-layer configuration is stabilized by the surface tension. As the centrifugal pressure Δp_ω head (1) increases, the liquid plug can move farther into the pneumatic chamber, thus making it harder for the surface tension to sustain the "hanging" liquid volume ΔV. At the so-called burst frequency, the liquid plug disrupts to invert the metastable liquid-gas configuration. Liquid thus proceeds into the pneumatic chamber to dissolve the DF membrane and hence open the valve.

For a given, rotationally induced pressure head Δp_ω (1), the distance the plug can protrude into the compression chamber (and the displaced air volume ΔV) until Δp_ω (1) balances the counter pressure p (2) increases with the dead volume of the chamber V_0. In other words, the fluidic capacitance defined volume change ΔV induced by a given pressure change p (2) increases with V_0. As the "burst" is induced towards increasing ΔV, the burst frequency shrinks with increasing chamber size V_0.

For a given (incompressible) liquid (ρ = const.), a chamber volume V_0, and plug volume, Δr cannot drastically be changed as a too wide channel would compromise the surface-tension dependent stabilization of the meniscus at the entrance of the DF chamber. Overall, the pressure head Δp_ω (1) is hence mainly controlled through $\bar{r}$, i.e. essentially the (fixed) radial position of the valve on the disc, and through its square dependence on the dynamically set angular frequency ω. For the work presented in this manuscript we will induce the valving condition $p_{crit} < \Delta p \sim \bar{r}\dot{\omega}$ (1) most often by ramping up ω. In section 7 dealing with sequential valving on the disc, valve triggering is demonstrated by raising ω as well as by jointly raising ω and $\bar{r}$.

4. Materials and methods

4.1 Device fabrication

In order to demonstrate our advanced, DF-assisted centrifugo-pneumatic valving concept, the multilayer tabs were integrated into a centrifugal microfluidic device. To begin with, the valving tabs were manufactured using a standard cutter-plotter machine (CraftROBO Pro cutter/plotter, Graphtec, USA). Through holes were first machined in double-sided PSA films. Next, the top carrier layer of the PSA was removed and the DF material was pressed to the exposed adhesive (PSA and DFs were acquired from Adhesives Research, Limerick, Ireland). A final cut was then performed to contour the complete assembly. The DF tabs could thus be manufactured in mass and premade for implantation into the microfluidic lab-on-a-chip devices when necessary.

The disc-based devices were created using established PSA/polymer lamination techniques.[18,19] To fabricate the rotor layers, large chamber features were laser machined (Zing 16 Laser, Epilog, USA) in 1.5-mm thick poly(methylmethacrylate) (PMMA, sourced from Radionics, Ireland) discs. Microfluidic channel features were defined in disc shaped 50–86 μm thick PSA layers using the same cutter plotter device as for the valving tabs (the same PSA material was also used to create the film tabs). The individual plastic and adhesive layers were sequentially stacked and tabs placed where necessary. The layers were machine pressed together to complete the final device.

4.2 Centrifugal microfluidic design

The design of the final disc incorporated several features necessary for centrifugo-pneumatic valving: an area for air trapping that included the 3D vial which created the air pocket region, a recess for receiving the plugs, as well as the DF tabs. In order to guide primary proof-of-principle experiments, a range of geometrical parameters was also set (e.g., radial placement of valve, radial length of the liquid plug, 3D vial diameter, and microchannel width) to replicate a conceivable valving situation (details of the dimensions can be found in the supplementary Figure S1.).

The DF plug design and tab placement in the disc was chosen in order to distinguish between valve dissolution and opening of the valve due to mechanical failure. A small through hole was centred within the 3D vial, so that after film dissolution, a small liquid retention pocket could be observed. In contrast, if mechanical failure occurred and the film broke free from the PMMA surface, no fluid was preserved in the pocket.

4.3 Experimental setup

Once a suitable design was established, a series of experiments was performed which targeted the burst frequency (BF) of the valve. The discs were placed on a spin stand setup, which contained a computer-controlled motor (Faulhaber Minimotor SA, Crogilio, Switzerland) that precisely modulated the rotational frequencies of the microfluidic device. In addition, this setup featured additional equipment that allowed for imaging during high-speed rotation. Using a sensitive camera (Pixelfly, PCO, Kehlheim, Germany) with motorized zoom optics (Navitar, Rochester, NY, USA) and a stroboscopic light source (Drelloscop 3244, Drello, Germany) the system allowed for the collection of one image of a defined area on the disc per rotation (details of a similar setup can be found in Grumann et al.[20]). The resulting images were then analysed, and measurements taken to evaluate the operation of the valving structure. It was of paramount importance to try to identify the critical BF where centrifugal forces cause the liquids to displace the trapped gas and open the valve. Additional trials using structures without plugs were run to establish negative controls for the system.

5. Results and discussions

5.1 System performance

The experiments demonstrated the centrifugo-pneumatic operating principle of our novel valving concept. Initially, a microfluidic design that did not incorporate a DF tab was first tested

(with no tab the feature functioned as a hydrophobic valve). In absence of a sacrificial barrier, fluids flowed unimpeded from the loading to the collection chamber at speeds of approximately 500 RPM. Next, a setup with identical features and the DF valve in place was investigated. In that design, low speed rotation propelled the sample from the loading chamber through the intake microchannel. However, the flow was stopped at the entrance of the air ballast compartment as expected from the centrifugo-pneumatic design concept. Rotational speeds were then increased at defined rates until the valve opened. The microfluidic experiments showed that the gas-liquid inversion did not occur instantaneously, but acted in a stepwise manner.

During acceleration, small droplets of liquid occasionally moved into the air ballast compartment. As the exposed film surface was located nearer to the centre of the chamber, the droplets were collected without prematurely opening the valve. Beyond a critical spinning rate, the gas-liquid interface fully destabilized, allowing for liquid to more fully fill the chamber and then contact the film surface. At this point film dissolution and valve opening occurred. An image series showing the progression of a sample test exhibiting the valving principle is depicted in Fig. 2C.

These experiments confirmed that the addition of the DF tabs dramatically increased the burst frequencies of the valves to a range that was not achievable with conventional capillary constrictions. Plugs that contained either the slow or quick dissolvable films maintain stability at rotational rates of approximately 3000 RPM as shown in Fig. 3. In this design, the measurement represented a rise in the burst centrifugal frequency by nearly a factor of 10. The notable increase in the burst frequency is important as the ability to maintain integrity at those high speeds is necessary for many fluidic processes, *e.g.*, centrifugally induced particle sedimentation.

In terms of actuation time, valves placed in the centrifugal system had limited dependence on the rated time dependency. In the disc, both the slow/quick dissolve tabs opened less than 10 s after contact; this roughly corresponds to the expected dissolution
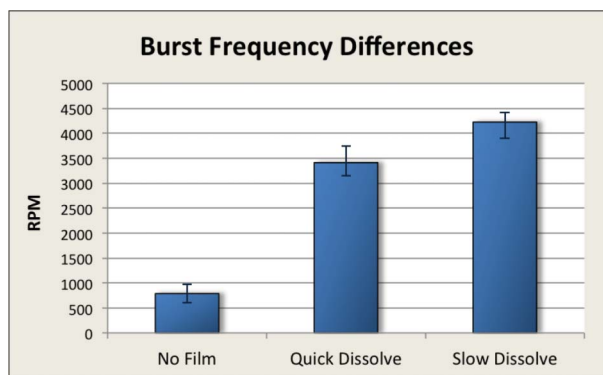

Fig. 3 Graph showing a dramatic increase in the burst frequency of the dissolvable film valves. Experimentation showed a 10-fold increase in valve stability with either the quick or slow dissolve films (*versus* a native hydrophobic valve at the same location) withholding fluids at above 3000 RPM. Error bars represent the range of opening speeds observed over a series of burst frequency experiments using discs with identical design structures.

time of the quick dissolve film (10 s) but much more rapidly than the rating of the slow dissolve film (5 mins). It is plausible that the active introduction of fluids to the film surface intensifies liquidation and accelerates valve opening. It should be noted that the rapid valve opening made pinpointing the exact operational RPM value difficult; this may have contributed to some of the observed error in the burst frequencies between the slow and quick dissolve films in Fig. 3. Regardless, the time-dependency of the films was greatly reduced, and as such, a range of films displaying various dissolution rates could be integrated easily. Future development could include adapting fluidic designs to take advantage of both frequency and dissolution times for valving.†

5.2 System evaluation

DF-based valving introduces a new development in microfluidic process control on centrifugal platforms. Foremost, the DF valve represents the first instance where it is possible to create a sacrificial barrier that is merely actuated by the rotation of the substrate intrinsic to the centrifugal platform, and thus eliminates the need for external actuation, like those required in laser ablation or heating-based techniques.[12,21,22] The vapour barrier properties of the DFs may also allow transient sealing and gating of liquid reagents for on-board storage.

In addition, the DF centrifugo-pneumatic concept improves on the previously introduced flexible burst seal valves, as DF valves allow free passage of liquids after opening and are capable of functioning at much higher rotational speeds (and thus operations required by such). Furthermore the DF valves avoid manufacturing activities associated with foils/polymers and PDMS/polymers. The design also improves on the original centrifugo-pneumatic system of Mark *et al.*[17] In that design, where a microchannel exits to a closed reservoir, the liquid shift into the gas pocket represents an endpoint operation. In contrast, the novel DF design creates an opening in the reservoir chamber. The DF system is capable of acting as an intermediate valving step connecting to subsequent liquid handling procedures. Moreover, as a consequence of the fabrication of the tabs, the valve is not dependent on the manufacturing process for the device. In terms of mass production, one could envision a pick-and-place manufacturing setup with prefabricated valves tailored to the specific use in the system.

6. Biocompatibility of dissolvable films

While the mechanical demonstration proved the potential for valving actuation on the disc, it was also important to verify that the films could be used with biological assays. Therefore, it was examined how the presence of the film affected the performance of molecular and immunoassays.

Mouse immunoglobulin variable genes were polymerase chain reaction (PCR) amplified in the presence and absence of the DFs. PCR amplification was performed according to protocols previously described (Barbas *et al.*).[23] The PCR reaction

---

† The valves retain their time-dependent nature in traditional "stationary" microfluidic systems. Figure S2 in the ESI shows a demonstration of DF valving in a straightforward 3D microvial using quick and slow dissolve film plugs. In that system the valves actuate near the film's rated dissolution times validating the rating from the manufacturer.

contained the following: 1 μl of murine cDNA, 60 pmol of forward and reverse oligonucleotide primers, 5x PCR buffer, 2-mM MgCl$_2$, 2.5-mM dNTPs and 0.25 μl Platinum® Taq DNA polymerase. Either quick or slow dissolve films were added to the PCR mix prior to processing. The PCR amplification profile was as follows: initial denaturation at 94 °C for 2 min, 30 cycles with denaturation at 94 °C for 15 s, annealing at 56 °C for 30 s, and extension at 72 °C for 90 s, followed by a final cycle of extension at 72 °C for 10 min. The amplicons were assessed using gel electrophoresis. No discernible differences in PCR amplification were observed when the dissolvable films were added to the PCR reaction *versus* the control (data shown in S3).

An immunoglobulin G (IgG) sandwich assay was also used to assess the biological effect of the dissolvable films. Human IgG (SeraCare Life Sciences, US) samples were analysed using both colorimetric and fluorescence based assay formats. MaxiSorp™ Immuno plates (Nunc) were coated overnight at 4 °C with 100 μL of protein A (10 μg mL^{-1}, Thermo Scientific, US). After washing with phosphate buffered saline solution (PBS, 150 mM, pH 7.4) plates were blocked with a 3% (v/v) solution of Bovine Serum Albumin (BSA, Jackson ImmunoResearch Laboratories, US) and incubated for 1 h at 37 °C. The plates were further washed and 100 μL of human IgG standards (50, 10, 2, 0.4, 0.08 and 0.016 μg mL^{-1}) diluted in either PBS, representing the control, or with either quick or slow dissolvable films added. In addition, a PBS only sample served as a negative control. The plate was then incubated for 1 h at 37 °C. After washing, 100 μL of an avian secondary (IgY) antibody against human IgG (Gallus Immunotech Inc., US) was applied, and the plate was incubated for 1 h at 37 °C. For the fluorescence assay, the plate was washed and 100 μL of a fluorescent Neutravidin-Dylight 649 complex (Thermo Scientific, US) was applied. The plate was incubated for 1 h at 37 °C and subsequently washed. After the addition of 100 μL of PBS, the fluorescence was measured using a commercial microplate reader (Tecan Safire2™). The excitation wavelength was 645 nm and the emission wavelength 675 nm. A similar procedure was used for colorimetric analysis except that, a 100 μL solution of horseradish peroxidase-labeled, avian, secondary antibody (Gallus Immunotech Inc., US) against human IgG was used for detection. After extensive washing bound antibody was detected by incubation with 3,3′ 5,5″-tetramethylbenzidine. After chromophore development, the reaction was stopped by the addition of 100 μL of 10% (v/v) HCl and the absorbance at 450 nm was measured with the same microplate reader.

Fig. 4 illustrates the resulting assay performance in the presence and absence of the dissolvable films. The black curve represents the normal assay without the addition of the dissolvable film. The blue curve shows the effect on the immunoassay when the quick dissolvable film is included. In contrast, the pink curve shows the effect on the immunoassay when the slow dissolvable film is introduced. Fig. 4A/B show that the dissolvable films do not negatively impact the performance of the immunoassays. In fact, when either the slow or quick dissolving films are added to the fluorescent or colorimetric immunoassays the respective fluorescence or absorbance signals are enhanced. In addition, there is a change in the slopes of the calibration curves, which results in a slight increase in assay sensitivity. The reason for such an effect is
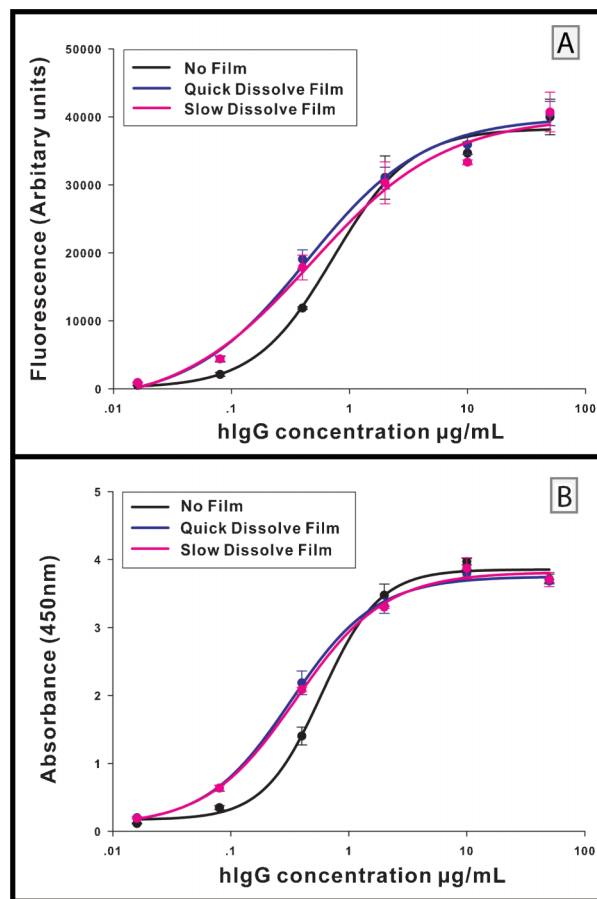

Fig. 4 Biocompatibility studies on the performance of dissolvable films on the human IgG Immunoassay. Variants of a similar test were developed for A) fluorescence based and B) colorimetric based analysis. Addition of either fast or slow dissolvable films did not negatively impact on the performance of the immunoassays

unknown. However testing of a series of negative controls (capture protein + film, capture protein + film + blocking agent, capture protein + film + blocking agent + detector, capture protein + film + blocking agent + analyte) did not reveal any significant increase in background signal. Therefore it does not appear that the dissolvable films by themselves increase either auto-fluorescence or color signal. It is plausible that one or more of the materials within the commercial proprietary dissolvable film enhances the analyte-antibody interaction and consequently increases the sensitivity of the immunoassay.

The PCR and sandwich immunoassay tests demonstrated the potential use of DFs for valving in bioassays. However, for applications including other molecular or protein targets, a biocompatibility assessment for each specific assay would be required. Additionally, cell-based assays would necessitate separate evaluation. Regardless, the current work verifies exploration of the technology and in particular the immunoassay experiments demonstrate that the films have potential applications beyond pure valving. For example, they could be used to store critical assay components. In essence, the valve would then become an advanced control element for liquid flow as well as a utility for on-board reagent storage.

7. Multiple valving operation

Valves play a critical role in facilitating complex flow control for the full integration and automation of complex bioassay protocols. In this manner, DF valving can also be used for more advanced sample processing. For instance, the retention of the valves at high-speeds shows potential for storing and withholding reagents throughout a series of spin protocols with opening on-demand at designated points in time. Such attributes are desirable, especially in applications like biomedical diagnostics where high-speed centrifugation is necessary. This is often the case in blood-based diagnostic assays where plasma separation from whole blood represents the critical initial assay processing step.

Valving is vital at this stage in integrated designs when dealing with blood for analysis; for example such assays require centrifugation to separate the blood constitutes of erythrocytes from plasma. In such a design, valves should initially retain regents/buffers required for analysis and subsequently process the components remaining in the supernatant. Therefore valves would that remain intact throughout high-speed centrifugation are required.

Fig. 5A/B shows a microfluidic design that demonstrates a set of DF valving structures. This system provides an example of a comprehensive design that would enable integrated analysis from whole blood. In each representative processing component, the valve implements the protocol features necessary to function or improves on the operation by allowing processing at higher RPM values. Fig. 5C–J demonstrate example assay steps with non-biological fluid samples. Of key importance is the fact that the DF-based valving introduced here allows the retention of prospective samples and reagents during fast centrifugal sedimentation at speeds well beyond the burst frequencies that could be achieved with capillary valves.

In brief, the device works by first enabling plasma separation through a typical disc-based decanting structure. In such designs a blood sample can be centrifugally separated in the loading chamber; the plasma is restricted using a DF valve to temporarily seal off a microchannel to the next processing chamber. To isolate the plasma layer, the disc is accelerated above the burst frequency of the first valve, allowing for controlled liquid removal (Fig. 5C–D). DF valves could thus replace the traditional plasma isolation method based on siphoning which has manufacturing issues around hydrophilic treatments[24] or requires the use of specialized hydrophilic surfaces.[25] In the next step of analysis, the sample liquid passes into another chamber where a centrifugal metering step is implemented (Fig. 5E). Fluid is restricted in a similar fashion as before, remaining in the chamber until accelerated past the burst frequency of a second DF valve (Fig. 5F) which then propels the
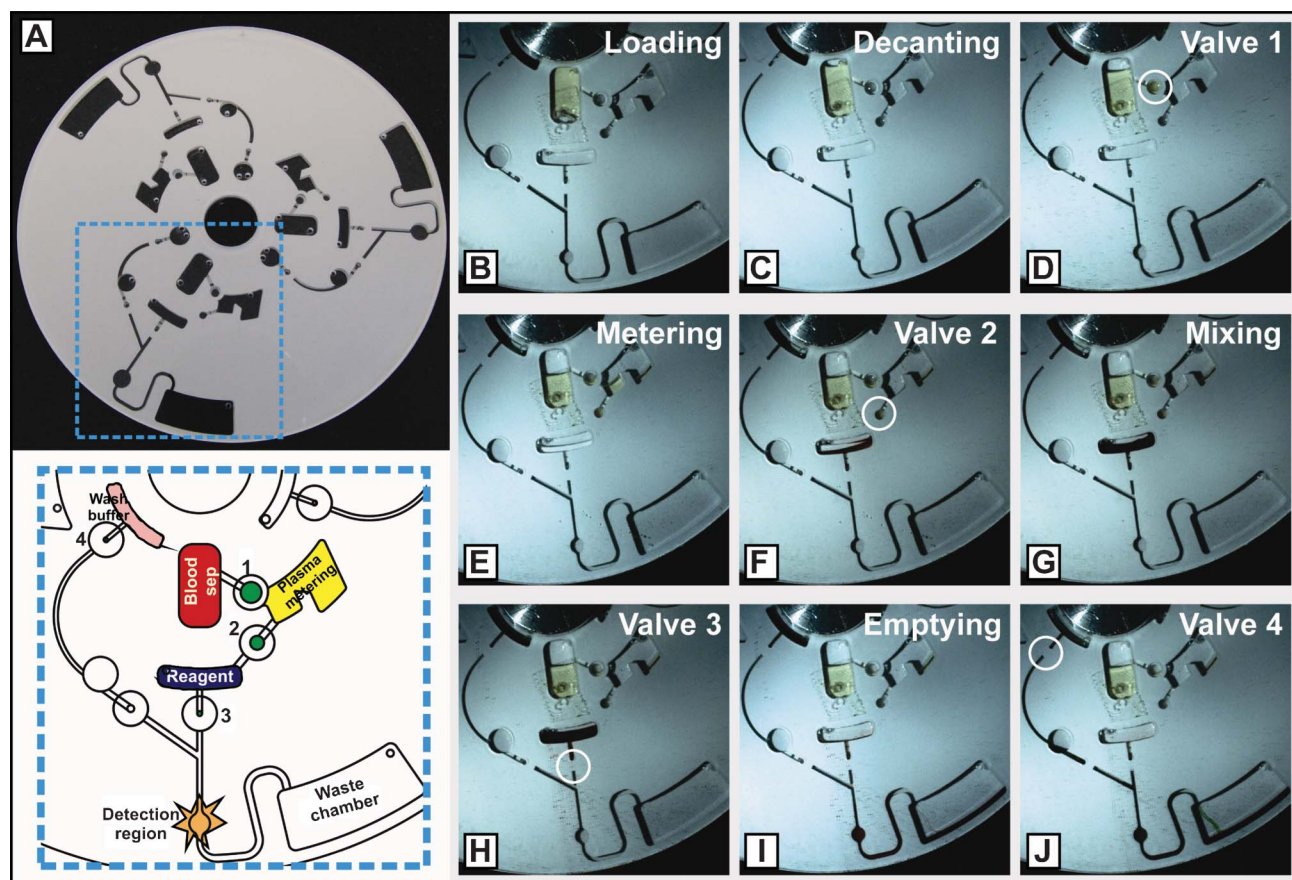

Fig. 5 Centrifugal microfluidic system with multiple DF valves outlining potential assay processing from whole blood. Note that non-clinical aqueous fluids were used to demonstrate sequential fluidic control. A) Image and schematic of the device profiling the fluidic designs (and potential fluidic functions) in the disc. B–J) Video stills demonstrating sequential fluidic control during operation of the disc.

liquid into a further mixing chamber. Although not fundamental to the mixing operation (which can be achieved using various techniques like batch processing or by shaking[26]), the valve increases the speeds and magnitude of the rotational acceleration in which mixing is preformed while preventing premature "leakage" of samples to subsequent processing areas (Fig. 5G). Two (or more) components can be vigorously agitated under high-amplitude accelerations rates by inhibiting any fluid flow. The mixture is then driven past a third valve and over a potential detection site, potentially functionalized with a capture reagent for the target analytes (Fig. 5H–I). Further acceleration breaks the final valve, and results in the release of a secondary reagent (for example a reagent with labelling chemistries or wash buffers) (Fig. 5J).

The operational protocol of the device is shown in Fig. 6A–C. This graph is colour–coded so as to demonstrate the correlation between the rotational burst frequency p_{crit} and pressure head Δp calculations (see Section 3.2) for each of the four DF valves labelled V1 to V4. Fig. 6C illustrates the sequence of the valve opening from V1 (decanting), V2 (metering), V3 (different stages of mixing) and V4 (wash buffer) before eventual detection. In Fig. 6A we plot the coefficient $\Delta p/\Delta p_{i,crit}$ which references the

pressure heads to the respective burst pressures of V1 to V4, *i.e.* each sequential crossing of the horizontal ($y = 1$)-line corresponds to a valve opening. Fig. 6B shows the calculated pressure head value of each of the DF valves. p_{crit} denotes the burst pressure that must be exceeded for each valve to actuate. It is important to note that when p_{crit} for one valve is reached, the pressure heads for all other operations remain well below their respective p_{crit} values. For example, at the time of 300 s, when $p_{1,crit}$ for V1 (decanting) is reached at 82 hPa, the pressure head for V2 (0 hPa), V3 (65 hPa) and V4 (33 hPa) all stay below this critical 82 hPa threshold. This further demonstrates the serial opening of the valves. Fig. 6C shows the experimentally determined rotational burst frequencies for the different valving operations.

Notice while the rotational burst frequency of V3 (2500 rpm) is lower than that of V2 of 3300 rpm (Fig. 6C), the burst pressure in Fig. 6B reveals that when $\Delta p_{2,crit}$ is reached, the $\Delta p_{3,crit}$ still remains sub-threshold. Although the addition of the sample into the mixing chamber increases the Δr and subsequently the pressure head in this chamber, the precise ramping down of the rotational frequency to ~600 rpm ensures that full mixing of potential plasma and reagent buffer occurs without letting liquid pass through V3. After proper mixing has occurred, the rotational frequency is then increased to 2500 rpm, thus actuating V3. The resulting V3 lower burst frequency of 2500 rpm is due to the increased Δr.

In general the DF-based centrifugo-pneumatic valve's ability to maintain durability at very high speeds allows for a suite of biological processing events to occur before valve opening. This could enable further integration in disc devices where reagents are withheld throughout high-speed spin protocols (*e.g.*, blood separation, cell/viral lysis, efficient reagent mixing) and released for further downstream processing in analysis and detection.

8. Conclusions

This report outlines the underlying working principle, assembly, and characterization of a novel centrifugo-pneumatic valving scheme, which is based on water-dissolvable films (DFs). The arrangement is unique in terms of valving in centrifugal microfluidic platforms, and is easily controlled by introducing the aqueous solutions to the substrate and allowing for film dissolution. The ability to simply integrate the valves in microfluidic devices is advantageous as compared to active valving, as the system can provide robust liquid and vapour seals while eliminating the need for peripheral actuation other than the innate spindle motor. In addition, the DF configuration expands the usable processing range (RPMs) of the burstable seal valves to enable comprehensive assay integration, automation and parallelization. The valves can be configured by adjusting the geometry of the system to various opening arrangements and have been proven for sequential liquid release and advanced processing.

In the context of diagnostic systems, biocompatibility studies showed that the films had no negative effects on the performance of either a PCR-based assay or colorimetric and fluorescence immunoassays. Furthermore, the dissolvable films could potentially be used to store liquid reagents above the valve (and even perhaps include reagents in the composition of the film itself).
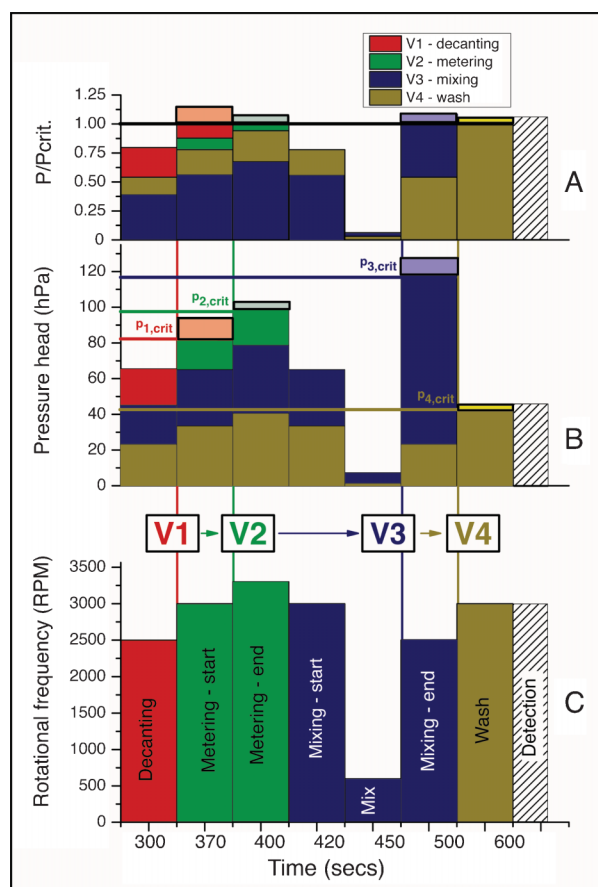

Fig. 6 Graph detailing the relationship between the pressure and the burst frequencies of the DF valves. A) Calibration graph of the coefficient of p/p_{crit}. Each sequential crossing of the horizontal $y = 1$ line corresponds to a valve opening. B) Pressure head graph for the DF valves. p_{crit} indicates the critical burst pressure that must be exceeded for each valve to actuate. C) Rotational burst frequency for each valving operation.

Overall, the system has high potential for advanced, high-pressure valving and reagent storage on the disc with low (lateral) footprint. Future work will include additional optimization of the design, continued biocompatibility validation for multiple biological analytes, and the eventual demonstration of fully integrated, multi-step assays utilizing such valves.

Acknowledgements

References

1 W. Meathrel and B. Meathrel, *IVD Technol*, 2007, **13**, 53–58.
2 R. Gorkin, J. Park, J. Siegrist, M. Amasia, B. S. Lee, J. M. Park, J. Kim, H. Kim, M. Madou and Y. K. Cho, *Lab Chip*, 2010, **10**, 1758–1773.
3 M. Madou, J. Zoval, G. Jia, H. Kido, J. Kim and N. Kim, *Annu. Rev. Biomed. Eng.*, 2006, **8**, 601–628.
4 J. Ducrée, S. Haeberle, S. Lutz, S. Pausch, F. von Stetten and R. Zengerle, *J. Micromech. Microeng.*, 2007, **17**, S103–S115.
5 S. Haeberle, T. Brenner, R. Zengerle and J. Ducrée, *Lab Chip*, 2006, **6**, 776–781.
6 J. Steigert, T. Brenner, M. Grumann, L. Riegger, S. Lutz, R. Zengerle and J. Ducrée, *Biomed. Microdevices*, 2007, **9**, 675–679.
7 H. Kido, M. Micic, D. Smith, J. Zoval, J. Norton and M. Madou, *Colloids Surf., B*, 2007, **58**, 44–51.
8 B. S. Lee, J. N. Lee, J. M. Park, J. G. Lee, S. Kim, Y. K. Cho and C. Ko, *Lab Chip*, 2009, **9**, 1548–1555.
9 P. Andersson, G. Jesson, G. Kylberg, G. Ekstrand and G. Thorsen, *Anal. Chem.*, 2007, **79**, 4022–4030.
10 D. D. Nolte, *Rev. Sci. Instrum.*, 2009, **80**, 101101.
11 J. Park, Y. K. Cho, B. Lee, J. Lee and C. Ko, *Lab Chip*, 2007, **7**, 557–564.
12 J. L. Garcia-Cordero, D. Kurzbuch, F. Benito-Lopez, D. Diamond, L. P. Lee and A. J. Ricco, *Lab Chip*, 2010, **10**, 2680–2687.
13 B. S. Lee, Y. U. Lee, H. S. Kim, T. H. Kim, J. Park, J. G. Lee, J. Kim, H. Kim, W. G. Lee and Y. K. Cho, *Lab Chip*, 2011, **11**, 70–78.
14 J. Hoffmann, D. Mark, R. Zengerle and F. von Stetten, *in Proceedings of Transducers*, Denver, CO, USA, 2009.
15 H. Hwang, H. H. Kim and Y. K. Cho, *Lab Chip*, 2011, **11**, 1434–1436.
16 C. Moritz, *Med. Design Technol*, 2006, **10**, 11–13.
17 D. Mark, P. Weber, S. Lutz, M. Focke, R. Zengerle and F. voin Stetten, *Microfluid. Nanofluid.*, 2011, **10**, 1279–1288.
18 J. Siegrist, R. Gorkin, M. Bastien, G. Stewart, R. Peytavi, H. Kido, M. Bergeron and M. Madou, *Lab Chip*, 2010, **10**, 363–371.
19 D. A. Bartholomeusz, R. W. Boutte and J. D. Andrade, *J. Microelectromech. Syst.*, 2005, **14**, 1364–1374.
20 M. Grumann, T. Brenner, C. Beer, R. Zengerle and J. Ducrée, *Rev. Sci. Instrum.*, 2005, **76**, 025101.
21 J. M. Park, Y. K. Cho, B. S. Lee, J. G. Lee and C. Ko, *Lab Chip*, 2007, **7**, 557–564.
22 K. Abi-Samra, R. Hanson, M. Madou and R. A. Gorkin, *Lab Chip*, 2011, **11**, 723–726.
23 C. F. Barbas III, D. R. Burton, J. K. Scott and G. J. Silverman, *Phage Display: A Laboratory Manual*. Cold Spring Harbor Laboratory Press: Cold Spring Harbor, New York, 2001.
24 A. Larsson and H. Dérand, *J. Colloid Interface Sci.*, 2002, **246**, 214–221.
25 J. L. Garcia-Cordero, L. Basabe-Desmonts, J. Ducrée and A. J. Ricco, *Microfluid. Nanofluid.*, 2010, **9**, 695–703.
26 M. Grumann, A. Geipel, L. Riegger, R. Zengerle and J. Ducrée, *Lab Chip*, 2005, **5**, 560–565.